IEEE Access
Multidisciplinary | Rapid Review | Open Access Journal

Received November 14, 2017, accepted February 19, 2018, date of publication February 27, 2018, date of current version March 16, 2018.

Digital Object Identifier 10.1109/ACCESS.2018.2809735

Running Experimental Research of a Wire Driven Astronaut Rehabilitative Training Robot

YUPENG ZOU[1], LIXUN ZHANG[2], LAILU LI[2], HUIZI MA[3], AND KAI LIU[1]

[1]College of Mechanical and Electronic Engineering, China University of Petroleum, Qingdao 266580, China
[2]College of Mechanical and Electrical Engineering, Harbin Engineering University, Harbin 150001, China
[3]College of Mathematics and System Science, Shandong University of Science and Technology, Qingdao 266590, China

Corresponding author: Yupeng Zou (zouyupeng@upc.edu.cn)

This work was supported in part by the National Natural Science Foundation of China under Grant 51705534, in part by the Fundamental Research Funds for the Central Universities under Grant 18CX02085A, and in part by the Shandong Provincial Natural Science Foundation under Grant ZR2016EEB12.

ABSTRACT Keeping astronauts physically healthy in the harsh space environment is a key to the successful execution of a space mission. Long-term space missions in the weightless environment, however, can result in space adaptation syndrome, which seriously affects astronauts' health. To alleviate the adverse effects, this paper proposes a wire driven astronaut rehabilitative training robot that simulates the characteristics of the gravity environment and load force on the astronauts. The robot can realize multiple physical exercises including running, bench press, and deep squat. A dynamic model of the wire driven unit (WDU) was provided. On this basis, a hybrid force controller was designed to improve the precision and real-time performance of WDU. Furthermore, a dual-closed-loop control strategy was proposed to improve the loading precision of the robot. Running experimental results demonstrate that the robot can load force safely and reliably during the physical training, and the control strategies are effective.

INDEX TERMS Astronaut rehabilitative training robot (ART), force control, space adaptation syndrome (SAS), weightless environment, wire driven.

I. INTRODUCTION

Manned spaceflight has facilitated many key discoveries about our universe as well as in-depth medical research about human physiology. During prolonged spaceflight, microgravity induces many adaptive and pathological changes within the human body, known as space adaptation syndrome (SAS), which are similar to changes that may occur in the elderly and bedridden patients [1]–[3]. All sorts of methods have been tried to relieve SAS, from drugs through psychological remedies to more outlandish treatments [4], [5]. Physical exercises have been taken as critical countermeasures to restore the cardiovascular function and protect the musculoskeletal system during prolonged spaceflight [6], [7]. Mitigating the impacts of SAS during spaceflight is important for astronauts to guarantee safety and to maintain their ability to perform extravehicular activities.

In earth's gravity environment, human beings can take high-intensity aerobic or anaerobic exercises to maintain or increase bone density and muscle strength [8]. Though the effectiveness of aerobic and anaerobic exercises during spaceflight is not entirely clear, crewmembers on International Space Station (ISS) spend approximately 5 hours on the aerobic exercises and 3-6 days on the anaerobic exercises per week [9]. Aerobic exercises are proposed as countermeasures to maintain cardiovascular function, muscle metabolism and neural response which have been performed primarily by using the cycle ergometer, the rower or the treadmill. Bicycling 30-120 min helps relieve the uncomfortable symptoms caused by cephalic fluid shift [10]. Treadmill with Vibration Isolation Stabilization System (TVIS), which can generate 1 g-like loads on the lower extremities, is designed to help astronauts prevent amyotrophia and osteoporosis [11]. Furthermore, it is important that the physical exercises during the spaceflight are effective and efficient. In addition they should be enjoyed by the astronauts. Therefore, anaerobic exercises, which reduce the training intensity and duration observably, have potential to serve as an effective countermeasure. Anaerobic exercises are the most effective countermeasures to maintain muscle mass and strength during prolonged spaceflight. For a long time, astronauts do anaerobic exercises with bungee, penguin suit or devices that provided limited resistance [12]. In November 2008,

NASA delivered a new Advanced Resistive Exercise Device (ARED) to ISS to replace the Interim Resistive Exercise Device (IRED). Compared with IRED, ARED is well accepted by the astronauts for its greater resistances and wider range of motions [13].

Each training device on ISS has its unique characteristics and unique functions. However, an investigation found that despite allocating approximately 2.5h per day for exercises, astronauts spent only 43min actually on physical training [14]. The remaining time was spent in repositioning and assembling the exercise devices. Existed exercise apparatuses have different assembly requirements which pose some challenges related to available training space on ISS and limited mission time of crewmembers.

To meet the special requirements of astronauts for a rehabilitative training robot with multiple training functions, small space occupation, easy operation and efficient comprehensive training effects, we have developed a novel wire-driven Astronaut rehabilitative Training Robot (ART) which integrate aerobic training (run) and anaerobic training (bench press, deep squat) in one equipment (Fig. 1). Essentially, ART is a modular and reconfigurable Wire-driven Parallel Robot (WDPR) which uses wires as the transmission components instead of the rigid linkage mechanism. WDPR features simple structure, high control precision, strong load adaptability, good flexibility and diversified operation modes. It can realize complex force/position control easily [15], [16].

To summarize, superiorities of applying WDPR to ART are: 1) modularization architecture can simplify ART's structure, reduce the difficulties in transportation and assembling, and cut down its space occupation; 2) the multimodal and reconfigurable characteristics make it possible to realize multiple forms of training on a single machine on ISS; 3) there is no rigid impact towards human body for the application of flexible wires which can improve the comfort of physical training; 4) to obtain better force control performance and simulate the gravity characteristic more closely, wires are driven by torque motors directly [17]–[19]. The rest of this paper is organized as follows. Section II characterizes the ART, including the robot design, mechanical structure analysis and Wire Driven Unit (WDU) design. The dynamic model of WDU is provided. Section III presents the control strategy. Section IV is dedicated to provide the experimental results. Conclusion and future work are given in Section V.

II. MECHANICAL STRUCTURE AND DYNAMICS MODELING

A. MECHANICAL STRUCTURE DESIGN OF ART

ART is a typical man-machine cooperation system which cannot work without the astronaut's participation. ART follows the active motion of the astronaut and exerts a gravity-like force on the astronaut during the physical exercise. Fig. 1 shows an overview of the three training modes that ART provides. Fig. 2 presents the overall mechanical part of ART. The configuration of ART mainly consists of six sets

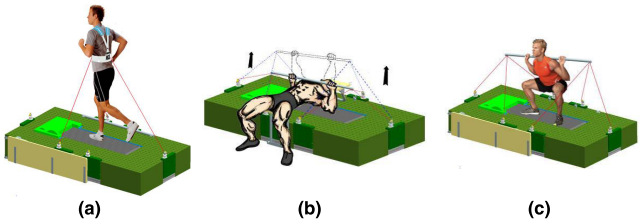

FIGURE 1. CAD model of the ART: (a) ART-aided run training, (b) ART-aided bench press training, and (c) ART-aided deep squat training.

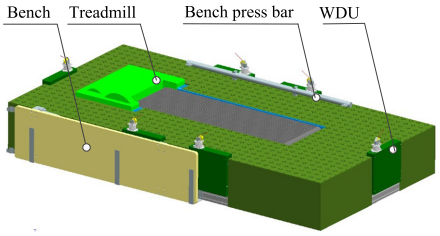

FIGURE 2. Mechanical part of ART.

of WDU which are symmetrically arranged on the frame. In addition, there is a bench, treadmill and bench press bar, etc.

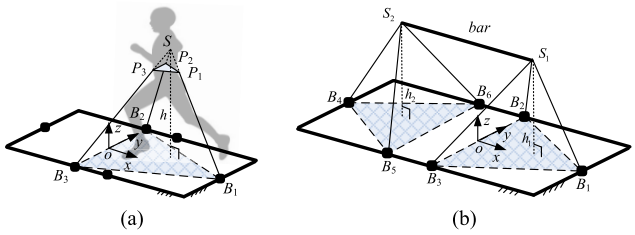

FIGURE 3. (a) Schematic diagram of ART-aided run training. (b) Schematic diagram of ART-aided bench press training and deep squat training.

The schematic diagrams of the three ART-aided training modes are presented in Fig. 3.

In the run mode, the astronaut's pelvis is loaded by three WDUs (Fig. 3(a)). While running on the treadmill, the human pelvis is a complex 6 DOF motion system. In these motions, the three-dimensional translations and the revolution around Z axis (about 5°) are the four fundamental factors that affect the stability and harmony of human-motion. Note that the triangle $\triangle P_1P_2P_3$ constructed by the three traction points is much smaller than the $\triangle B_1B_2B_3$ constructed by three WDUs ($\triangle P_1P_2P_3 \backsim \triangle B_1B_2B_3$). In actual operation, the variations of the wire-length caused by the pelvic Z-rotation can be neglected and the motion of pelvis can be approximately regarded as translational motion [20]. It is easy to prove that the inner tensions of the three wires (B_1P_1, B_2P_2 and B_3P_3) can constitute a spatial concurrent force system. A vertically downward resultant force can be acquired at the point S by controlling the wires' inner tensions.

Similarly, in the bench press and the deep squat mode, each end of the bar (point S_1 and point S_2) is loaded by three WDUs to simulate the gravity of the barbells (see

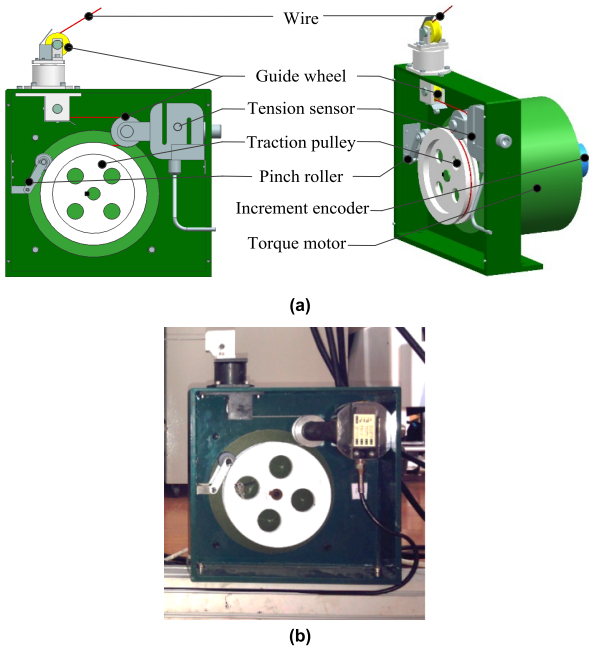

FIGURE 4. (a) The 3D-model of the WDU. (b) The prototype of the WDU.

Fig. 3(b)). Every point is loaded by a spatial concurrent force system.

B. MECHANICAL STRUCTURE DESIGN OF WDU

Fig. 4 illustrates the composition of the WDU. The WDU consists of a torque motor that drives a traction pulley directly. An increment encoder is located on the motor and the encoder's readings are used to determine the wire elongation. The pose state and localization of the bar or the pelvis can be further determined. A pinch roller, fixed on the side frame, is used to confine the wire to the traction pulley groove. A tension sensor is fixed on the other side of the frame and a guide wheel is located on the opposite part of the tension sensor. After passing through the guide wheel, the wire's motion direction changes 180°. The tension of the sensor is twice as much as the wire. Finally, the wire connects to the target after passing through a fixed guide wheel and a rotating guide wheel.

Compared with the high-speed DC motor, the low-speed torque motor can work under the locked-rotor state continuously. Besides, a reducer can be saved by using the torque motor and the bad effect of the gear clearance to the force control performance can be eliminated.

The assembly of the tension sensor has the following characteristics: 1) Fixed-installation of the sensor can improve the measurement accuracy. If the tension sensor move along with the wire, the measurement result F would be seriously influenced by the inertial force of the tension sensor ($F = f + \xi + ma$, f is the wire tension, ξ is the sensor noise, ma is the inertial force of the tension sensor). 2) The tension sensor is pulled by two wires. In case of measuring the same wire tension, fixed-installation of the sensor can reduce the proportion of sensor noise in the measurement result $F = (2f+\xi)/2$.

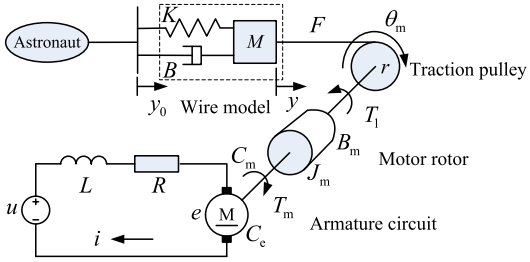

FIGURE 5. The mechanism model of WDU.

C. DYNAMIC MODEL OF WDU

Based on the composition and characteristics of the WDU, the mechanism model of the WDU is shown in Fig. 5. The WDU transfers the force to the astronaut through the wire. To clarify the effect of the wire more clearly, the wire can be simplified into a mass-spring-damping model for its low vibration frequency in the training process.

According to Fig. 5, the armature circuit equation of the DC torque motor is

$$L\frac{di}{dt} + Ri + e = u \tag{1}$$

where $e = C_e\dot{\theta}_m$.

The torque equilibrium equation can be described as

$$T_m = T_l + J_m\ddot{\theta}_m + B_m\dot{\theta}_m \tag{2}$$

where $T_m = C_m i$.

The force equilibrium equation of the mass-spring-damping model is

$$F - B(\dot{y} - \dot{y}_0) - K(y - y_0) = M\ddot{y} \tag{3}$$

Besides,

$$T_l = Fr \tag{4}$$

$$y = \theta_m r \tag{5}$$

According to the (1)-(5), the block diagram of the WDU is shown in Fig. 6. The wire tension F is influenced by two inputs: the motor armature voltage u and the position disturbance y_0 caused by the movement of the astronaut.

According to Fig. 6, the mathematical model of the WDU force servo system is

$$F(s) = M_1(s)U(s) - M_2(s)V_0(s) \tag{6}$$

In (6), V_0(s) is the velocity of the traction point, $V_0(s) = sY_0(s)$.

M_1(s) is the transfer function from the input voltage u to the output force F. It's the transfer function of forward channel.

$$M_1(s) = \frac{C_m r(Ms^2 + Bs + K)}{J_e L s^3 + (B_e L + J_e R)s^2 + (B_e R + C_m C_e + KLr^2)s + KRr^2} \tag{7}$$

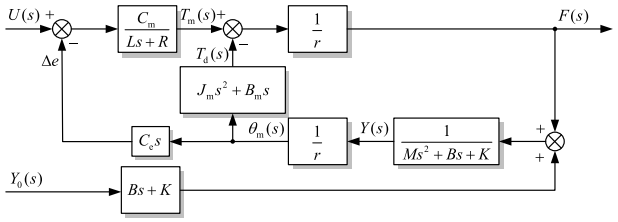

FIGURE 6. Block diagram of WDU.

$M_2(s)$ is the transfer function from the input velocity disturbance v_0 to the output surplus force F. It's the transfer function of disturbance channel.

$$M_2(s) = \frac{(Bs+K)[J_{\mathrm{m}}Ls^2+(B_{\mathrm{m}}L+J_{\mathrm{m}}R)s+(B_{\mathrm{m}}R+C_{\mathrm{m}}C_{\mathrm{e}})]}{J_{\mathrm{e}}Ls^3+(B_{\mathrm{e}}L+J_{\mathrm{e}}R)s^2+(B_{\mathrm{e}}R+C_{\mathrm{m}}C_{\mathrm{e}}+KLr^2)s+KRr^2} \tag{8}$$

In (7) and (8), $J_{\mathrm{e}} = Mr^2 + J_{\mathrm{m}}$ is the equivalent moment of inertia, $B_{\mathrm{e}} = Br^2 + B_{\mathrm{m}}$ is the equivalent viscous friction coefficient.

III. CONTROL STRATEGY

A. HYBRID FORCE CONTROL STRATEGY OF WDU

In the training process, the WDUs passively follow the active movement of astronaut and exert a desired resultant force on the astronaut [21]–[23]. For each WDU, it's a force servo system, or rather a typical passive force servo system. The control strategy design for the passive force servo system should consider two aspects: (a) To improve the response speed and precision of the force control, a forward channel compensator should be designed based on the forward channel transfer function $M_1(s)$. (b) To minimize the negative impact of the velocity disturbance v_0, a surplus force compensator should be designed. The hybrid force control strategy for the wire driven passive force servo system is shown in Fig. 7. The forward channel compensator consists of an integral link, a local negative feedback link $G_{p\_lead}(s)$, and a feed-forward link $G_{ff}(s)$. The surplus force compensator $G_{cv}(s)$ is designed based on the structure invariance principle.

To improve the steady-state accuracy, the integral link is used as the primary controller of the forward channel which improves the system from 0-type to I-type. However, a single integral link will decrease the phase reserve and lower the dynamic quality.

In this case, the local negative feedback link $G_{p\_lead}(s)$ (a second order phase-lead link), composed of a proportional link K_a, a second order oscillation link and a second order differentiation link, can be used to improve the system's dynamic quality.

$$G_{p\_lead}(s) = K_a \frac{\frac{s^2}{\omega_{\mathrm{an}}^2} + 2\xi_{\mathrm{an}}\frac{s}{\omega_{\mathrm{an}}} + 1}{\frac{s^2}{\omega_{\mathrm{ad}}^2} + 2\xi_{\mathrm{ad}}\frac{s}{\omega_{\mathrm{ad}}} + 1} \tag{9}$$

Under the premise of ensuring stability, the feed-forward link $G_{ff}(s)$ in combination with the local negative feedback link $G_{p\_lead}(s)$ can enhance the response speed of the force servo system. Essentially $G_{ff}(s)$ is a proportional link. When the input $F_d(s)$ changes rapidly, the primary controller response slowly for the integral link has an significant attenuation influence on input signals. Meanwhile, the input $F_d(s)$ transmit to the phase-corrected system by dint of $G_{ff}(s)$. The force servo system works in the open-loop state approximately and the response speed of system can be brought into play adequately. When the force servo system reaches a stable state, the impact of the integral link will be gradually shown out. The steady-state accuracy will be improved.

The surplus force compensator $G_{cv}(s)$ is designed on the basis of phase-corrected system that corrected by the local negative feedback link $G_{p\_lead}(s)$. This will simplify the designing of the surplus force compensator and avoid the influence of high-order differential component.

$$G_{\mathrm{cv}}(s) = \frac{M_2(s)}{G_{p\_lead}(s)M_1(s)} \tag{10}$$

B. DUAL CLOSED LOOP CONTROL STRATEGY OF ART

To ensure ART can provide training services effectively and safely, a dual closed loop control strategy is adopted in robot control (Fig. 8). The inner controller refers to the hybrid force controller for the wire driven passive force servo system. The outer controller (the master control system) is responsible for resultant force control, tension planning, safety monitoring, etc.

The working principle of the dual closed loop control strategy is as follows. The master control system implements the tension planning and determines the desired wire tensions f_{di} according to the training programs, the desired resultant force and the position-pose state of the astronaut. The position-pose state of the astronaut is indirectly determined by the lengths of the wires l_{i} (detected by the encoders). Each WDU follows the input instruction f_{di} under the control of the hybrid force controller and applies the tension on the astronaut. Then the actual resultant force exerts on the astronaut can be confirmed according to the actual wires' tension f_i. The master control system further modifies the desired wire tensions f_{di}.

IV. RUNNING EXPERIMENTAL EVALUATION

A. EXPERIMENTAL PROTOCOL

A preliminary experiment was conducted to evaluate the effectiveness of ART in terms of force loading performance during the run training. The experiment was carried out in the gravity environment. One healthy subject participated in the experiment.

Fig. 9 shows the experimental setup of the running test. The man-machine prototype system mainly includes a subject, three WDUs, a treadmill, an accelerometer, a safety harness, a host computer with dSPACE and three sub computer control modules (STM32F107).

In order to test the real effect of ART, the subject was required to conduct 1 min uninterrupted running on the treadmill under different conditions. The experiments were

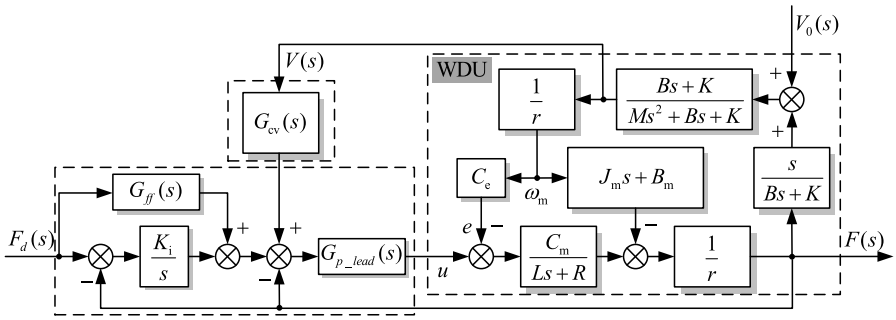

FIGURE 7. Hybrid force control strategy for the wire driven passive force servo system.

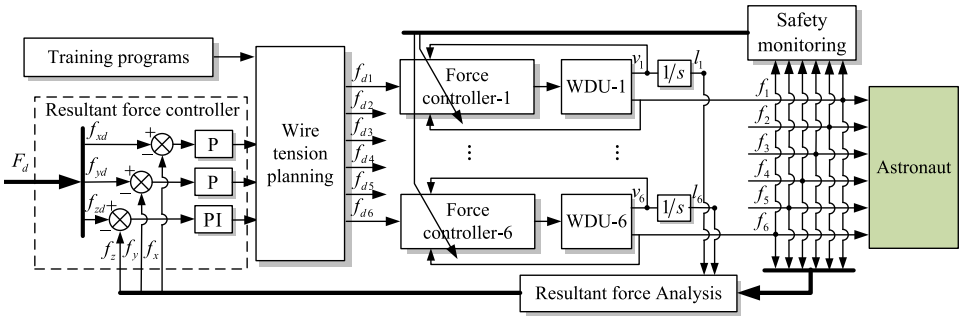

FIGURE 8. The control diagram of ART.

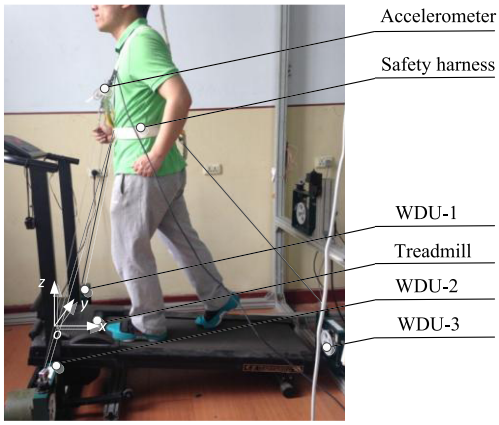

FIGURE 9. Experimental setup of the running test.

firstly carried out under different speed conditions (2.5 m/s and 4 m/s). Furthermore, two experiments were carried to check the effects of the surplus force compensator and the resultant force controller.

The virtual mass M_0 that ART needed to simulate was set at 10 Kg to ensure the safety and comfort of the subject in the running process. The virtual gravitational acceleration g was set at 10 m/s^2. The vertical acceleration of the subject a could be detected by the accelerometer. Then the desired resultant force f_d was

$$f_d = G_0 + M_0 a \tag{11}$$

In the training sessions, the subject was required to run as naturally as possible. Several trials served as practice for the subject to get familiar with the experiment protocol. The experimenter started collecting data after confirm with the subject that he could run comfortably with the robotic assistance.

B. EXPERIMENTAL RESULTS ANALYSIS

1) SPEED 2.5 m/s

The subject was equipped with the robot and ran on the treadmill. Set the speed of the treadmill at 2.5 m/s. Fig. 10 shows experimental results in the running experiment to illustrate the performance of ART.

As shown in Fig. 10 (a), the actual vertical downward resultant force f essentially agrees with the desired resultant force f_d and the actual resultant force f is much smoother. This illustrates that ART can provide the sense of gravity environment for the subject.

Fig. 10 (b) shows the transversal forces in the running process. The amplitude of the x directional transversal force f_x is approximately 4N. The amplitude of the y directional transversal force f_y is approximately 2N. The transversal forces cannot affect the normal running.

As shown in Fig. 10 (c) and Fig. 10 (d), the wire speed curves and the vertical acceleration curve have the characteristic of periodic fluctuation during the running process. This suggests that the running process is sustained and stable. This is in accordance with the actual process. Furthermore, due to the pelvis's translational motion in the horizontal direction, the speed curves of the WDUs have differences on the amplitude. The phase relation, however, is approximately consistent.

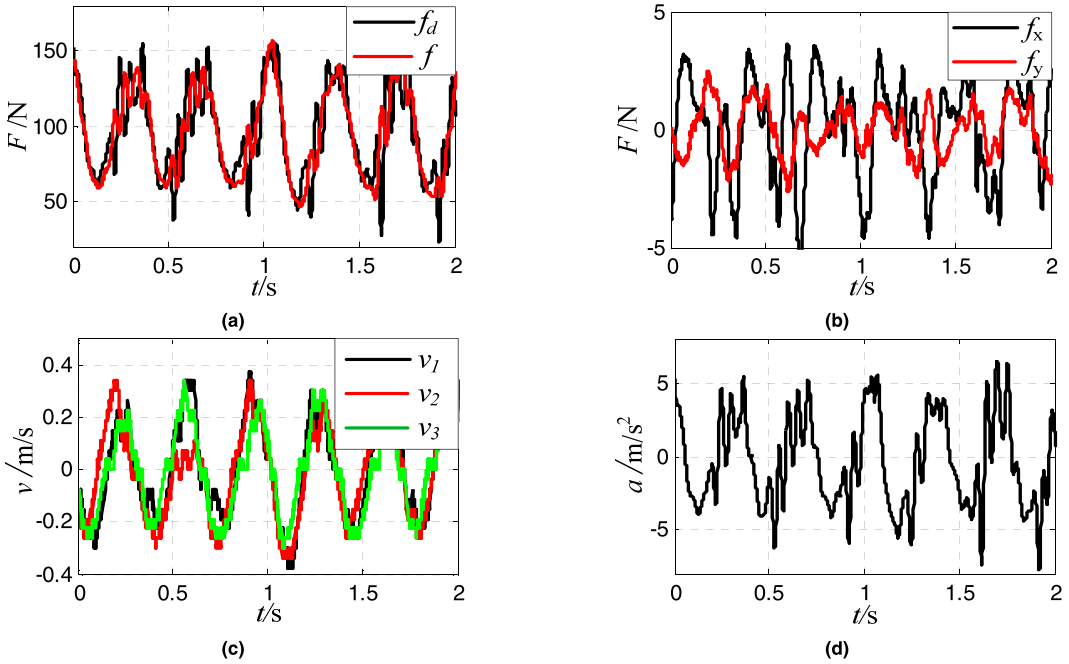

FIGURE 10. Results of the running experiment at the speed of 2.5 m/s: (a) desired vertical downward resultant force f_d and actual resultant force f; (b) transversal forces f_x and f_y; (c) wire speed curves of WDU1, WDU2 and WDU3; and (d) vertical acceleration of the subject during the running experiment.

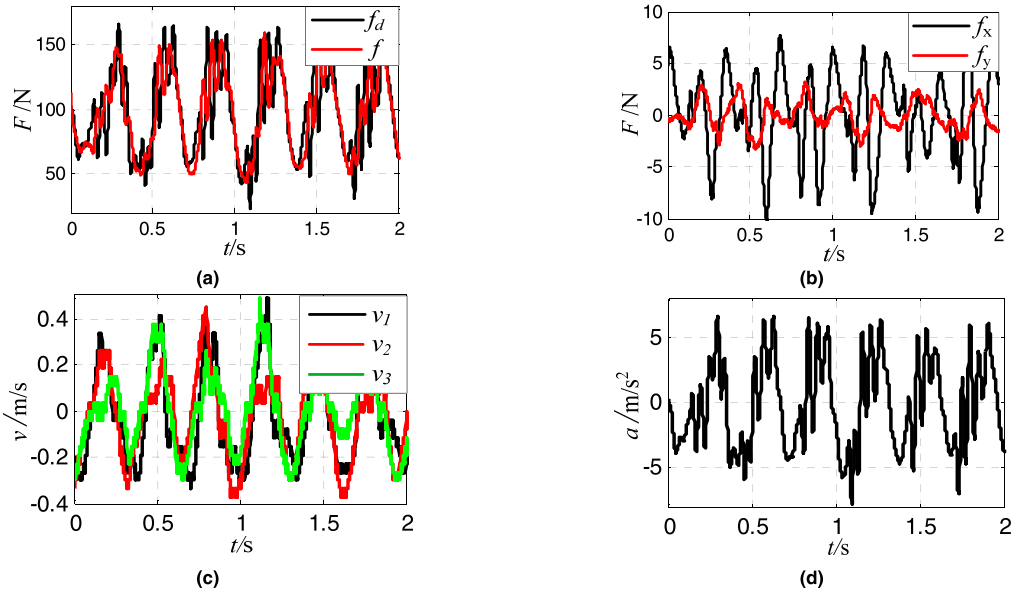

FIGURE 11. Results of the running experiment at the speed of 4.0 m/s: (a) desired vertical downward resultant force f_d and actual resultant force f; (b) transversal forces f_x and f_y; (c) wire speed curves of WDU1, WDU2 and WDU3; and (d) vertical acceleration of the subject during the running experiment.

2) SPEED 4.0 m/s

In order to verify ART's reliability in the state of running at high speed, set the speed of the treadmill at 4.0 m/s. Fig.11 shows the experiment performance of ART.

With the improving of the running speed, the subject's stride length and stride turnover improve correspondingly, and the running process is stable. In Fig. 11 (a), it can be seen that the actual vertical downward resultant force f still agrees with the desired resultant force f_d. The desired resultant force f_d increases with the increasing of the vertical acceleration. The transversal forces also have the enhancement ($f_x \approx 7$N, $f_y \approx 3$N), but still have little impact on the normal running (see Fig. 11 (b)). In Fig. 11(c) and Fig. 11(d), the wire speed and the vertical acceleration, which still have their own regularity, increase slightly.

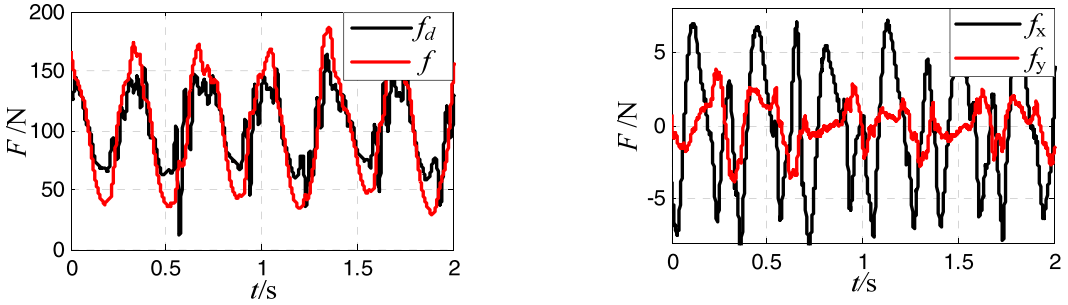

FIGURE 12. Experiment without resultant force controller: (a) desired vertical downward resultant force f_d and actual resultant force f; and (b) transversal forces f_x and f_y.

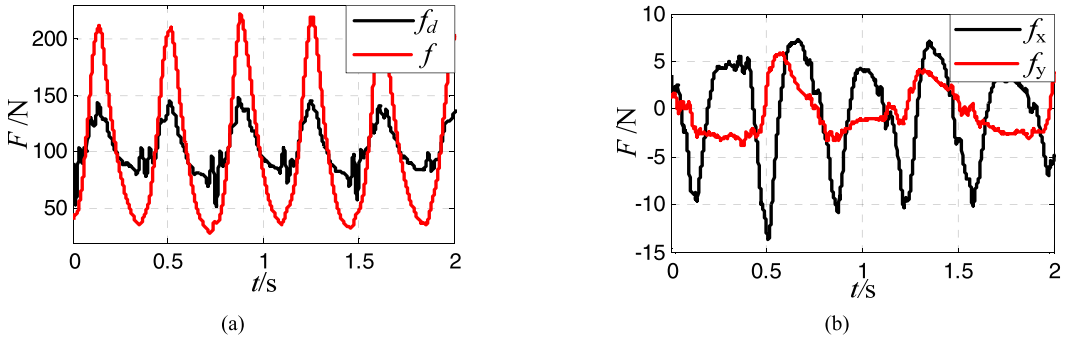

FIGURE 13. Experiment without resultant force controller and surplus force compensator: (a) desired vertical downward resultant force f_d and actual resultant force f; and (b) transversal forces f_x and f_y.

3) CONTRAST EXPERIMENTS

To check the effects of the resultant force controller and the surplus force compensator, two contrast experiments were carried out. Set the speed of the treadmill at 2.5 m/s. Fig. 12 and Fig. 13 show the experimental performance of ART. In both cases, the control accuracy of the vertical downward resultant force is obviously descended, and there are obvious increases in the transversal forces. The performance of ART cannot meet the training demand, and the security of the subject might be compromised.

In conclusion, the experiment results demonstrate that an excellent force loading performance was obtained during the run training. The actual vertical downward resultant force essentially agreed with the desired resultant force, and the transversal forces were partly suppressed. More importantly, the subject managed to maintain a natural running posture with the aid of the robotic device. We can infer that the ART can realize multiple physical exercises including running, bench press and deep squat, and help the astronauts to alleviate the adverse impact caused by SAS.

V. CONCLUSION AND FUTRUE WORK

In this paper, we present the mechanical design and experimental evaluation of a wire-driven astronaut rehabilitative training robot aimed for astronauts to carry out multiple physical exercises in the weightless environment. The dynamic model of WDU was provided. On this basis, we designed a hybrid force controller for WDU and a dual-closed-loop control strategy for ART. Running trials demonstrated that the robot can load force safely and reliably during the physical training.

As part of our continuing work, we are working on control methodologies for the robot to improve the force control accuracy and reduce the transversal forces. We are also developing a new prototype to decrease the weight and volume of the WDU, which makes the transportation and installation easier. A virtual zero-gravity environment will be built and experiments will also be conducted to further evaluate the effectiveness of the robotic system.

REFERENCES

[1] W. E. Thornton and F. Bonato, "Space motion sickness and motion sickness: Symptoms and etiology," *Aviation Space Environ. Med.*, vol. 84, no. 7, pp. 716–721, 2013.

[2] G. Clément and J. T. Ngo-Anh, "Space physiology II: Adaptation of the central nervous system to space flight–past, current, and future studies," *Eur. J. Appl. Physiol.*, vol. 113, no. 7, pp. 1655–1672, 2013.

[3] T. H. Mader *et al.*, "Optic disc edema, globe flattening, choroidal folds, and hyperopic shifts observed in astronauts after long-duration space flight," *Ophthalmology*, vol. 118, no. 10, pp. 2058–2069, 2011.

[4] T. Streeper *et al.*, "Development of an integrated countermeasure device for use in long-duration spaceflight," *Acta Astron.*, vol. 68, nos. 11–12, pp. 2029–2037, 2011.

[5] J. M. Waldie and D. J. Newman, "A gravity loading countermeasure skinsuit," *Acta Astron.*, vol. 68, nos. 7–8, pp. 722–730, 2011.

[6] A. E. Aubert, F. Beckers, and B. Verheyden, "Cardiovascular function and basics of physiology in microgravity," *Acta Cardiol.*, vol. 60, no. 2, pp. 129–151, 2005.

[7] A. LeBlanc *et al.*, "Bone mineral and lean tissue loss after long duration space flight," *J. Musculoskeletal Neuronal Interactions*, vol. 1, no. 2, pp. 157–160, 2000.
[8] A. R. Hargens, R. Bhattacharya, and S. M. Schneider, "Space physiology VI: Exercise, artificial gravity, and countermeasure development for prolonged space flight," *Eur. J. Appl. Physiol.*, vol. 113, no. 9, pp. 2183–2192, 2013.
[9] S. Trappe *et al.*, "Exercise in space: Human skeletal muscle after 6 months aboard the international space station," *J. Appl. Physiol.*, vol. 106, no. 4, pp. 1159–1168, 2009.
[10] H. Akima, N. Hotta, K. Sato, K. Ishida, T. Koike, and K. Katayama, "Cycle ergometer exercise to counteract muscle atrophy during unilateral lower limb suspension," *Aviation Space Environ. Med.*, vol. 80, no. 7, pp. 652–656, 2009.
[11] S. M. Smith *et al.*, "Evaluation of treadmill exercise in a lower body negative pressure chamber as a countermeasure for weightlessness-induced bone loss: A bed rest study with identical twins," *J. Bone Mineral Res.*, vol. 18, no. 12, pp. 2223–2230, 2003.
[12] G. Clement, "The maintenance of physiological function in humans during spaceflight," *Int. Sportmed J.*, vol. 6, no. 4, pp. 185–198, 2005.
[13] R. E. Nash *et al.*, "Muscle volume increases following 16 weeks of resistive exercise training with the advanced resistive exercise device (ARED) and free weights," in *Proc. ACSM 56th Annu. Meeting*, Seattle, WA, USA, 2009, p. 1.
[14] P. R. Cavanagh, K. O. Genc, R. Gopalakrishnan, M. M. Kuklis, C. C. Maender, and A. J. Rice, "Foot forces during typical days on the international space station," *J. Biomech.*, vol. 43, no. 11, pp. 2182–2188, 2010.
[15] Y.-P. Zou, L.-X. Zhang, H.-Z. Ma, and T. Qin, "Hybrid force control of astronaut rehabilitative training robot under active loading mode," *J. Central South Univ.*, vol. 21, no. 11, pp. 4121–4132, 2014.
[16] L. Zhang, L. Li, Y. Zou, K. Wang, X. Jiang, and H. Ju, "Force control strategy and bench press experimental research of a cable driven astronaut rehabilitative training robot," *IEEE Access*, vol. 5, pp. 9981–9989, 2017.
[17] M. Gouttefarde, "Characterizations of fully constrained poses of parallel cable-driven robots: A review," in *Proc. 32nd Annu. Mech. Robot. Conf.*, 2009, pp. 21–30.
[18] G. Rosati, P. Gallina, and S. Masiero, "Design, implementation and clinical tests of a wire-based robot for neurorehabilitation," *IEEE Trans. Neural Syst. Rehabil. Eng.*, vol. 15, no. 4, pp. 560–569, Dec. 2007.
[19] Y. Mao and S. K. Agrawal, "Design of a cable-driven arm exoskeleton (CAREX) for NEURAL rehabilitation," *IEEE Trans. Robot.*, vol. 28, no. 4, pp. 922–931, Aug. 2012.
[20] B. Zi, G. Yin, and D. Zhang, "Design and optimization of a hybrid-driven waist rehabilitation robot," *Sensors*, vol. 16, no. 12, p. 2121, 2016.
[21] X. Wang, S. Wang, and P. Zhao, "Adaptive fuzzy torque control of passive torque servo systems based on small gain theorem and input-to-state stability," *Chin. J. Aeron.*, vol. 25, no. 6, pp. 906–916, 2012.
[22] W. Chengwen, J. Zongxia, S. Yaoxing, and W. Zeng, "Suppress surplus torque based on velocity closed-loop synchronization," in *Proc. Int. Conf. Fluid Power Mechatronics*, Beijing, China, Aug. 2011, pp. 435–439.
[23] M. Karpenko and N. Sepehri, "Electrohydraulic force control design of a hardware-in-the-loop load emulator using a nonlinear QFT technique," *Control Eng. Pract.*, vol. 20, no. 6, pp. 598–609, 2012.

YUPENG ZOU received the B.S. and Ph.D. degrees from the College of Mechanical and Electrical Engineering, Harbin Engineering University, Harbin, China, in 2009 and 2014, respectively. He is currently a Lecturer with the College of Mechanical and Electrical Engineering, China University of Petroleum, Qingdao, China. His research interests mainly include rehabilitation robots and cable driven robots.

LIXUN ZHANG received the B.S. and M.S. degrees from the College of Mechanical and Electrical Engineering, Harbin Engineering University, Harbin, China, in 1984 and 1987, respectively, and the Ph.D. degree from the School of Mechatronic Engineering, Harbin Institute of Technology, Harbin, in 1994. He is currently a Professor of mechanical engineering with the Harbin Engineering University. He has authored 3 books, over 200 articles, and over 30 inventions. His research interests include collaborative robots, rehabilitation robots, surgical robots, and wind turbines.

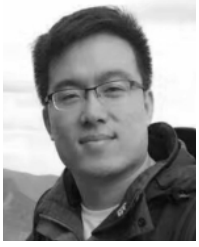

LAILU LI received the B.S. degree from the School of Mechatronic Engineering, China University of Mining and Technology, Xuzhou, China, in 2012. He is currently pursuing the Ph.D. degree in mechanical engineering at the Harbin Engineering University, Harbin, China. His current research interests include rehabilitation robots and cable driven parallel robots.

HUIZI MA received the B.S. and Ph.D. degrees from the School of Economics and Management, Harbin Engineering University, Harbin, China, in 2009 and 2014, respectively. She is currently a Lecturer with the College of Mathematics and System Science, Shandong University of Science and Technology, Qingdao, China. Her research interests mainly include stochastic control and backward stochastic differential equations.

KAI LIU received the B.S. degree in mechanical and electrical engineering from Shandong Agricultural University, Tai'an, China, in 2014. He is currently pursuing the M.S. degree in mechanical engineering at the China University of Petroleum, Qingdao, China. His research interests include cable driven robots and control system design.